Angle of Arrival Estimation Using Decawave DW1000 Integrated Circuits

Igor Dotlic, Andrew Connell, Hang Ma, Jeff Clancy, Michael McLaughlin
Decawave Ltd., Adelaide Chambers, Peter Street, Dublin 8, Ireland,
Email: first_name.last_name@decawave.com

***Abstract*—The paper describes principles of angle of arrival estimation using an anchor and a tag which are built around Decawave's DW1000 impulse radio ultra-wideband IC. Typical experimental results are provided that show the performance of Decawave's AOA demo kit based on this architecture.**

Keywords—Angle of arrival (AOA); Impulse Radio (IR); Ultra-Wideband (UWB); Real Time Localization System (RTLS).

I. INTRODUCTION

DW1000 [1, 2] integrated circuit (IC) represents a fully coherent implementation of the IEEE 802.15.4a [3] ultra-wideband (UWB) physical layer (PHY), which is currently integrated in the IEEE 802.15.4-2015 standard [4]. The impulse nature of this PHY along with its large bandwidth allow for precise real-time localization system (RTLS) implementation based on the DW1000 IC.

Up until now, the academic community made several contributions based on the DW1000 RTLS evaluation kits provided by Decawave. Comparison of the ranging performances of DW1000 evaluation kit and similar evaluation kits from other vendors has been done in [5-7]. Testing novel localization concepts with DW1000 ICs has been performed in [8], while experimenting with channel-sounding functionality of DW1000 ICs has been reported in [9].

This paper presents an overview of how to implement an Angle of Arrival (AOA) solution using Decawave's DW1000 IC with a Phase Difference of Arrival (PDOA) scheme. It also describes Decawave's initial AOA demonstration kit, based on Decawave's AOA anchor board, which is still under development. Furthermore, typical AOA estimation results using this kit are provided together with the description of its current limitations.

II. THEORETICAL BACKGROUND

A. Angle of Arrival Estimation Methods

Using Impulse Radio Ultra-Wideband (IR-UWB) technology such as in DW1000, four schemes can be used to calculate the angle of arrival from an IR-UWB source (tag) transmitting to two IR-UWB receivers (anchor):

- Time of Flight (TOF) [*where delta between two measured times of flight values is used to estimate angle. TOFs are estimated by two separate two-way ranging procedures* [10].].
- Time Difference of Arrival (TDOA) [*where delta between receive timestamps of the same frame is used to estimate angle*].
- Phase Difference of Arrival (PDOA) [*where delta between phases of the received carrier is used to estimate angle for the same frame*].
- TDOA/PDOA hybrid [*where, for distances between antennae above half-wavelength, TDOA is used to select one of pre-defined AOA intervals and PDOA is used to get the AOA estimate within the selected interval*].

For DW1000-based AOA solutions, PDOA gives the highest accuracy of the angle estimate and this is the scheme that will be used here. However, it is worth noting that Decawave also has experience with AOA estimation solutions based on TDOA/PDOA hybrid scheme. This is why this scheme will be briefly introduced.

B. PDOA AOA Estimation Method Principles

Consider a radio signal sent from a distant transmitter which arrives at two antennas. This is shown in Figure 1. It can be seen from the geometry depicted in Figure 1 that the difference in path length (p) is related to the distance between antennae A and B (d) and the angle of arrival (θ) as

$$p = d\sin(\theta). \tag{1}$$

Consider a signal wavelength $\lambda = 2\pi c/f$, where f is its carrier frequency and c denotes the speed of light. Then, PDOA (α) is related to p and λ (or f) as

$$\alpha = \frac{2\pi}{\lambda}p = \frac{f}{c}p. \tag{2}$$

Hence, from (1) and (2) relation between PDOA and AOA is derived as

$$\theta = \arcsin\frac{\alpha\lambda}{2\pi d}. \tag{3}$$

The above equation is derived assuming antennae A and B having identical radiation patterns, which can be only achieved if the effects of mutual coupling are negligible. Moreover, from (3) it is clear that, in order for α and θ to have one-to-one mapping in $\theta = [-\pi/2\,, \pi/2]$ interval, $d < \lambda/2$ has to hold.

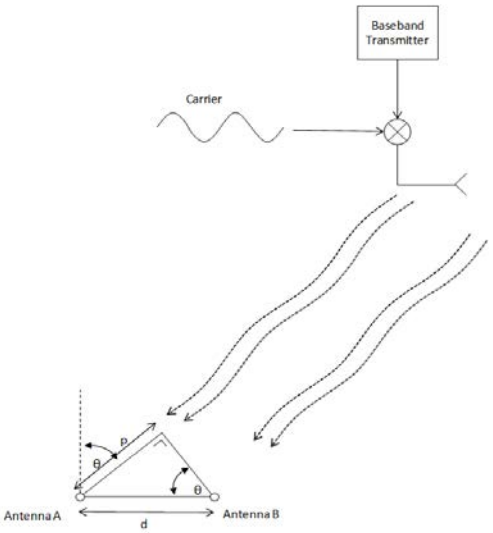

Figure 1: Principles of AOA estimation.

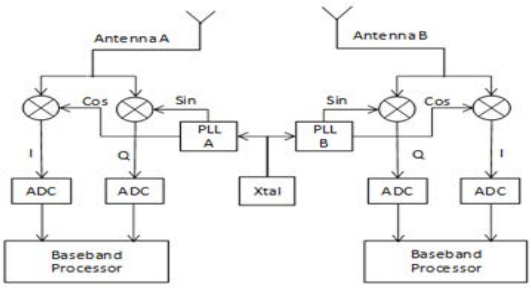

Figure 2: DW1000 scheme used to estimate AOA.

At such antennae distances, mutual coupling is rather significant. Therefore, care has to be taken in the design of AOA estimation antenna arrays in order for such effects to be relatively small. Furthermore, the channels to each antenna element are not linear phase channels and will introduce group delay and phase delay.

C. Advantages of Using UWB in AOA Estimation

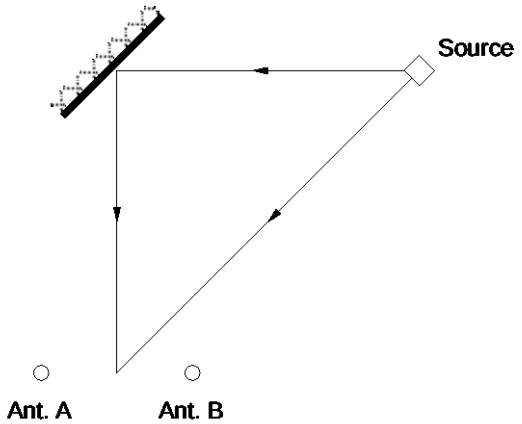

Figure 3: Space-time channel used in the example.

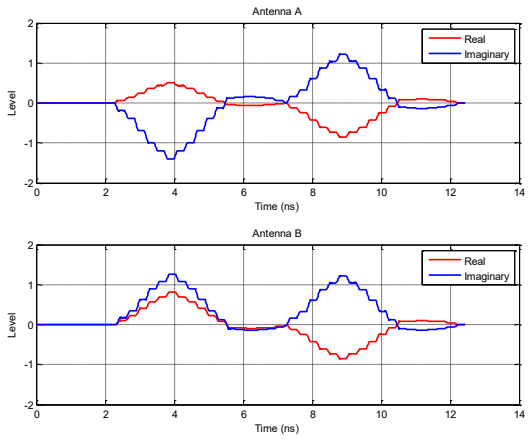

Figure 4: Received signal at antennae A and B in the complex baseband.

Since the signal bandwidth is not a part of (3), it would seem that PDOA scheme explained above can be used in both narrowband and UWB systems with equal success. However, as we will show now, there is a significant advantage of UWB over narrowband when using this method.

Let us consider two-ray space-time channel model depicted in Figure 3 with two receiving antennas spaced half wavelength apart at $f = 6.5$ GHz carrier frequency (2.31 cm). The first path impinges with 45° AOA and the second path impinges with 0° AOA. TOA difference between paths is 5 ns and, for our purposes, they have the same level at the receiver. An IEEE802.15.4a compliant UWB pulse is transmitted from the source. In the baseband domains of the two receivers shown in Figure 2 this pulse produces I and Q signals depicted in Figure 4.

It is clearly visible from Figure 4 that UWB receivers are capable of path separation due to the large bandwidth of the UWB pulse, i.e. its short duration. This is the reason why PDOA of the first path can be precisely measured by using a coherent UWB radio. If a narrowband signal is transmitted instead, the received pulses would be considerably wider and thus the paths would not be separated. In other words, narrowband PDOA and thus AOA estimation is very prone to error due to multipath. Similarly, due to its much higher path separation capability, UWB is much more resilient to multipath fading in comparison to narrowband systems.

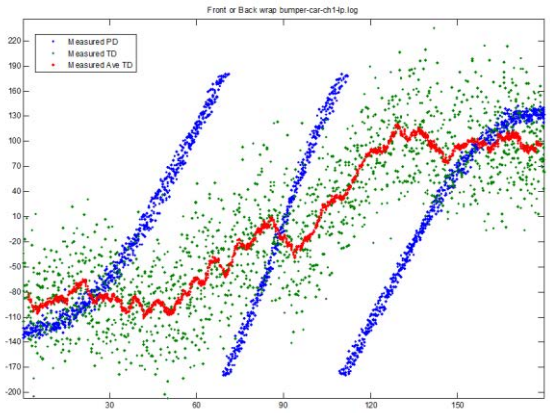

Figure 5: Typical performance of TDOA/PDOA hybrid method.

D. Principles of TDOA/PDOA Hybrid Method

By looking at the received first path pulses depicted in Figure 4, it is clear that their PDOA at 45° AOA is significant (127°) and, hence, easy to measure. On the other hand, their TDOA is only 54 ps which is much smaller than the inherent measurement error. This is an illustration of the general fact that getting AOA estimate from TDOA is much less precise than getting it from PDOA with antenna separations below half-wavelength.

The precision of an AOA estimate made from a TDOA measurement can be increased by increasing the antenna spacing, since this increases the TDOA for any given AOA. Nevertheless, as illustrated in Figure 5, the maximum TDOA is still relatively low at three half-wavelength spacing. At this antenna spacing the PDOA sensitivity to changing AOA is also increased, as also shown in Figure 5. On the other hand, the one-to-one mapping between AOA and PDOA is lost (3). This is the basis of the TDOA/PDOA hybrid AOA estimation method: Three possible AOAs are calculated from the PDOA, then TDOA is used to decide which solution is correct. Depending on the expected TDOA error, it may be necessary to average two or more TDOA estimates. Note that careful antenna design is required if using this method. It is essential that the differential group delay versus AOA is a constantly increasing function.

E. DW1000 Scheme Used to Estimate AOA

Figure 2 shows two receivers (2 x DW1000) which are clocked from the same crystal. Because they have the same crystal clocking an identical PLL, the generated carriers that are supplied to both of the down converter mixers will have the same phase. The radio signal will arrive at a slightly later time at antenna A than antenna B, so it will encounter a different down converter carrier phase in the mixer (1), (2). If the baseband processors are capable of calculating the complex impulse response of the channel, that impulse response will have a different I/Q relationship which is equal to the phase delay caused by the signal travelling an extra distance p, before encountering the mixer and being down-converted by the carrier.

F. AOA Calculation Method

Decawave has a patent pending method of estimating AOA using phase difference of arrival. This method can be implemented using 2 x DW1000 ICs clocked from the same 38.4 MHz reference clock input. Each DW1000 is connected to an antenna and the antennas are optimally separated by approximately *λ/2*. Using this hardware set up the phase difference (and hence angle of arrival) between the signals received at each antenna can be calculated.

Simplified phase difference calculation method is as follows:

1. When a frame is received, read the first path index from each DW1000 (A and B) and the complex sample from accumulator at first path (FP) index rounded to the nearest integer.
2. Get FP angles of A and B, denoted ϕ_A and ϕ_B, respectively.
3. Get synchronization frame delimiter (SFD) [4] angles of A and B, denoted β_A and β_B, respectively.
4. Calculate α in $[-\pi, +\pi]$ interval as

$$\alpha = \big((\phi_A - \beta_A - \phi_B + \beta_B + \pi) \bmod 2\pi\big) - \pi. \quad (4)$$

5. Get θ from α as

$$\theta = \frac{1}{0.95} \arcsin \frac{\alpha}{\pi}. \quad (5)$$

The above formula differs from (3), but fits well with the results obtained using the anchor antenna array chosen for Decawave's AOA demonstration kit. In other words, (5) gives good model of non-ideal effect described in Sec. B for the antenna array used. In the measurement results α that satisfies (5) for some given θ will be referred to as "Real PDOA".

PDOA measurement is widely used for AOA estimation (see e.g. [11-13]). However, novelty of the above method lies in the way the PDOA is extracted from a received IEEE 802.15.4a UWB PHY frame. Namely, here the whole complex channel impulse response is separately estimated at two receivers and respective FP indices are independently found. For each receiver, respective phase of arrival (POA) is calculated as a difference of its FP phase and its SFD phase. Then, the PDOA is calculated as a difference of the two POAs (4).

III. Decawave's AOA Demonstration Kit

A. Overview

Decawave has developed an initial prototype AOA demonstration kit. This kit is still under development. Decawave can provide early technology access to selected customers. Decawave will support these customers to develop solutions for their application and to get feedback to improve the demonstration kit performance.

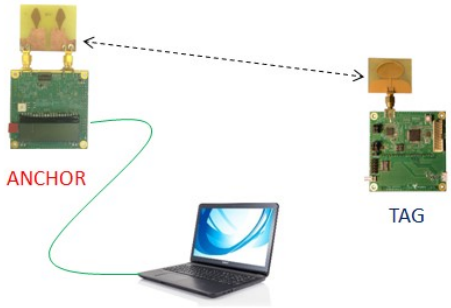

Figure 6: AOA demonstration kit contents.

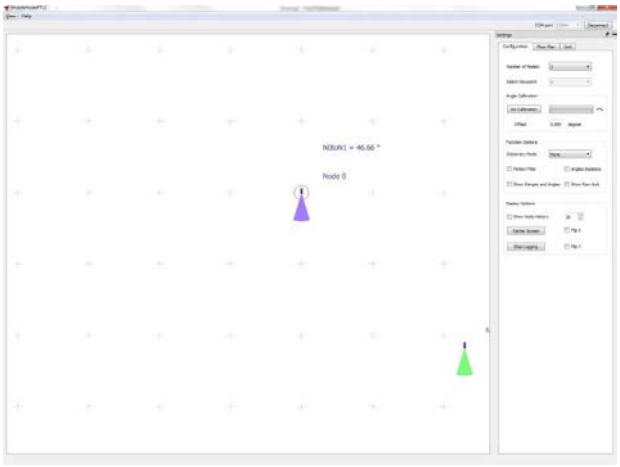

Figure 7: AOA demo GUI.

B. *Kit Contents*

Figure 6 shows contents of the Decawave's AOA demonstration kit. The kit contains anchor evaluation board and tag evaluation board with appropriate cables, antennas and software. Antennas delivered within the kit may differ from those shown in the figure. Furthermore, the antennas may be integrated with the boards in the future.

C. *What the Kit Does*

Two-way ranging is used [10] to estimate the distance between the tag and the AOA anchor. During the ranging process, the AOA anchor can also extract the angle estimate. The AOA anchor can then output the range and angle estimates for the tag. These outputs are made available on a UART interface.

A GUI is also supplied where the location and movement of the tag can be shown on a grid, as illustrated in Figure 7.

IV. Typical Results

A. *Experimental Setup*

The measurements were performed with the anchor placed on a turn table, which is located inside a small anechoic chamber. The tag was located on a stand outside of the chamber at a distance of 1.6 m from the anchor. The elevation of the stand can be adjusted, as well as the orientation of the tag.

B. *Tag Antenna Orientation*

The orientation of the tag antenna is characterized by its pitch roll and yaw. The meaning of these terms is illustrated in Figure 8, where x-axis represents the line-of-sight between the tag and the AOA anchor for zero degrees yaw and pitch.

C. *Zero Roll, Yaw, Pitch and Elevation*

The results for different azimuth AOAs, are shown in Figure 9. For this example, the tag antenna and the AOA anchor antenna array are in the same horizontal plane, i.e. elevation of the tag is zero. Moreover, pitch, roll and yaw of the tag are all zero.

It is visible in this figure that for positive AOAs above 80 degrees the estimation error is rather high. Moreover, for 90 degrees AOA the estimated angle becomes negative, which is seen as "jumping" to negative angles in the GUI. Figure 10 shows measured PDOA in this scenario.

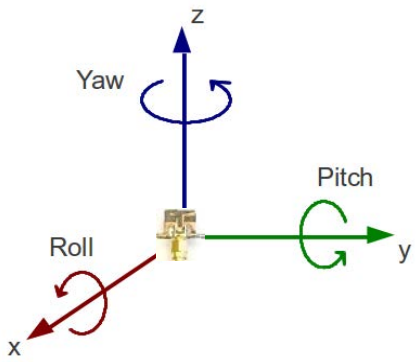

Figure 8: Pitch, roll and yaw of the tag.

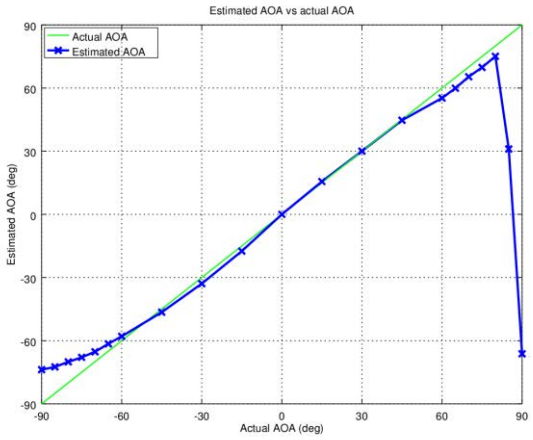

Figure 9: Typical estimated AOA performance vs actual AOA for zero elevation, pitch, roll and yaw.

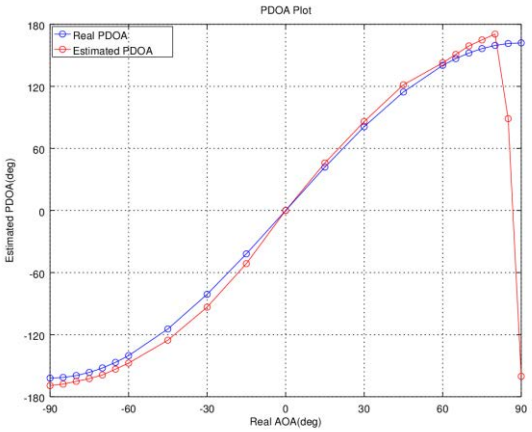

Figure 10: Typical measured PDOA performance vs azimuth AOA for zero elevation, pitch, roll and yaw.

D. Altering Tag Pitch, Roll and Yaw

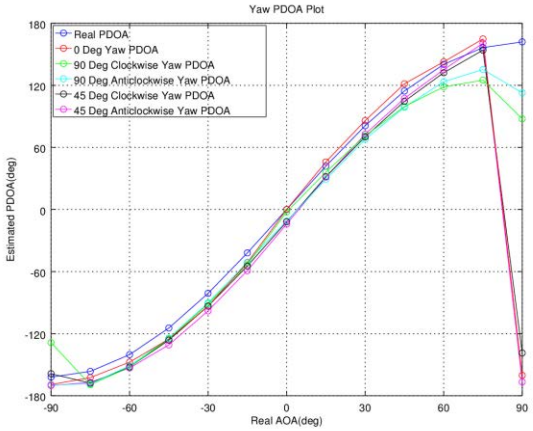

Figure 11: Typical measured PDOA performance vs azimuth AOA with different tag antenna yaw angles.

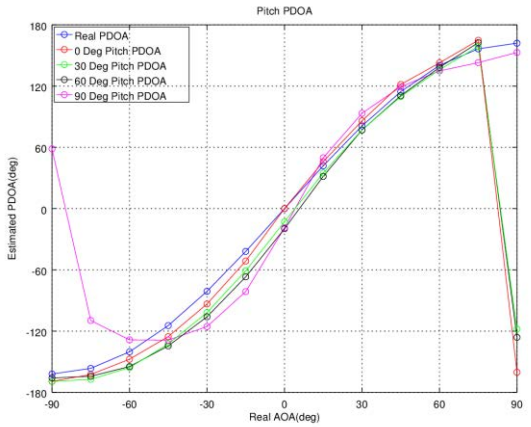

Figure 12: Typical measured PDOA performance vs azimuth AOA with different tag antenna pitch angles.

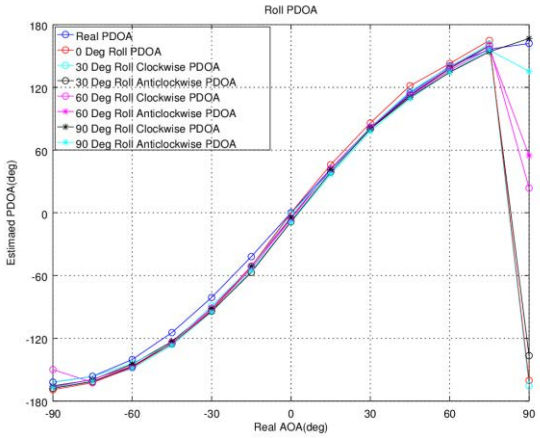

Figure 13: Typical measured PDOA performance vs azimuth AOA with different tag antenna roll angles.

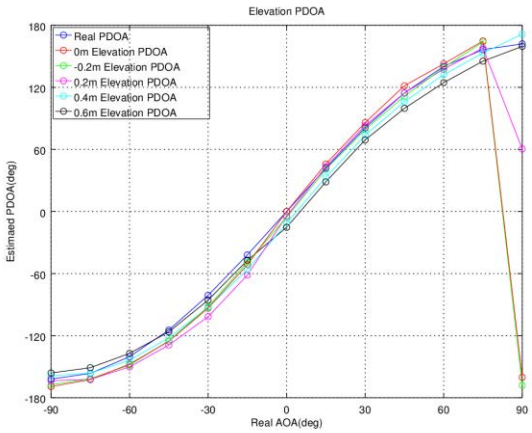

Figure 14: Typical measured PDOA performance vs azimuth AOA with different tag elevations.

Figure 11, Figure 12 and Figure 13 show typical results for tag yaw, pitch and roll, respectively. It is visible from these Figs that the kit is relatively resilient to the tag orientation changes.

E. Altering Tag Height

The measurements shown in Figure 14 present considerable amount of resilience of the azimuth angle estimation to the tag elevation variations.

V. KIT LIMITATIONS

A. Azimuth Angle Range

The azimuth range for which AOA can be successfully estimated is up to ±80 degrees in the front half-hemisphere of the AOA anchor, due to the electromagnetic limitations of the anchor antenna array. The anchor antenna array is not designed to estimate AOA in its back half-hemisphere.

B. Azimuth Angle Estimation Accuracy

For this combination of the tag and the anchor antennae, the PDOA saturates for negative angles with high absolute values,

whereas it jumps for high positive angles. The error of the tag azimuth angle estimation vs actual azimuth angle is shown in Figure 15. The accuracy of the estimation may be somewhat improved for high absolute values of the AOA by using an appropriate look-up table instead of the PDOA to AOA conversion formula (5).

C. Tag Elevation

As noted above, the measurements shown in Figure 14 show considerable amount of resilience of the azimuth angle estimation to the tag elevation variations. Nevertheless, the recommended AOA antenna array has two elements. As such, theoretically, it can measure the angle in only one dimension. This dimension is the plane that is defined by the AOA anchor array elements' positions and the tag position. When translated to spherical coordinates, this angle, denoted θ_p, is related to the tag azimuth angle (θ) and the tag elevation angle (φ) as

$$\sin\theta_p = \sin\theta\cos\varphi. \qquad (6)$$

This fact limits the possibility of estimating the tag azimuth angle for arbitrary elevation angle, which is required in many applications. For estimating the spatial angle (azimuth and elevation angle) of the tag more complex array geometries are needed with at least three elements.

VI. Conclusions

The proposed AOA anchor architecture based on the DW1000 ICs proved to be capable of high quality first path PDOA estimation. The design proved to be fairly robust to changing tag orientation (pitch roll and yaw), as well as changing the tag elevation. Furthermore, the kit has relatively small AOA estimation errors for AOAs in ± 80 degrees interval. The source of these errors are described electromagnetic effects at the anchor antenna array, rather than the inability of the anchor board to correctly measure PDOA.

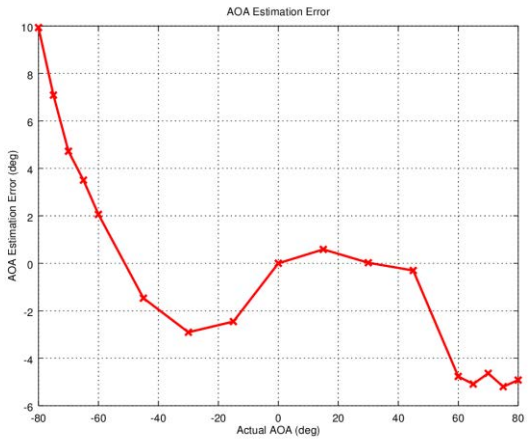

Figure 15: AOA estimation error vs actual AOA.

References

[1] *DW1000 Datasheet V2.12.*, Decawave. [Online]. Available: http://-decawave.com/

[2] D. Neirynck, *An IEEE 802.15.4a Ultra-Wideband Transceiver for Real Time Localization and Wireless Sensor Networks*. Cham: Springer International Publishing, 2014, pp. 297–310. [Online]. Available: http://-dx.doi.org/10.1007/978-3-319-01080-9_17

[3] *IEEE Standard for Information Technology - Telecommunications and Information Exchange Between Systems - Local and Metropolitan Area Networks - Specific Requirement Part 15.4: Wireless Medium Access Control (MAC) and Physical Layer (PHY) Specifications for Low-Rate Wireless Personal Area Networks (WPANs)*, IEEE 802 Std., 2007.

[4] *IEEE Standard for Low-Rate Wireless Networks*, IEEE 802 Std., April 2016.

[5] A. R. Jiménez and F. Seco, "Comparing Decawave and Bespoon UWB location systems: Indoor/outdoor performance analysis," in *2016 International Conference on Indoor Positioning and Indoor Navigation (IPIN)*, Oct 2016, pp. 1–8.

[6] A. R. J. Ruiz and F. S. Granja, "Comparing Ubisense, BeSpoon, and DecaWave UWB Location Systems: Indoor Performance Analysis," *IEEE Transactions on Instrumentation and Measurement*, vol. PP, no. 99, pp. 1–12, 2017.

[7] J. Wang, A. K. Raja, and Z. Pang, "Prototyping and Experimental Comparison of IR-UWB Based High Precision Localization Technologies," in *2015 IEEE 12th Intl Conf on Ubiquitous Intelligence and Computing and 2015 IEEE 12th Intl Conf on Autonomic and Trusted Computing and 2015 IEEE 15th Intl Conf on Scalable Computing and Communications and Its Associated Workshops (UIC-ATC-ScalCom)*, Aug 2015, pp. 1187–1192.

[8] J. Kulmer, S. Hinteregger, B. Großwindhager, M. Rath, M. S. Bakr, E. Leitinger, and K. Witrisal, "Using DecaWave UWB transceivers for high-accuracy multipath-assisted indoor positioning," in *2017 IEEE International Conference on Communications Workshops (ICC Workshops)*, May 2017, pp. 1239–1245.

[9] A. Moschevikin, E. Tsvetkov, A. Alekseev, and A. Sikora, "Investigations on passive channel impulse response of ultra wideband signals for monitoring and safety applications," in *2016 3rd International Symposium on Wireless Systems within the Conferences on Intelligent Data Acquisition and Advanced Computing Systems (IDAACS-SWS)*, Sept 2016, pp. 97–104.

[10] Decawave. Aps013: Dw1000 and two way ranging. [Online]. Available: https://www.decawave.com/support

[11] Z. Wang, W. Xu, and S. A. Zekavat, "A New Multi-Antenna Based LOS - NLOS Separation Technique," in *2009 IEEE 13th Digital Signal Processing Workshop and 5th IEEE Signal Processing Education Workshop*, Jan 2009, pp. 331–336.

[12] D. Manteuffel, T. Ould, and T. Kempka, "Antenna and propagation impairments of a UWB localization system integrated into an aircraft cabin," in *2010 Loughborough Antennas Propagation Conference*, Nov 2010, pp. 589–592.

[13] Z. Chen, G. Gokeda, and Y. Yu, *Introduction to Direction-of-Arrival Estimation*, ser. Artech House signal processing library. Artech House, 2010.